



Stability of amorphous drug, 2-benzyl-5-(4-chlorophenyl)-6-[4-(methylthio)phenyl]-2H-pyridazin-3-one, in silica mesopores and measurement of its molecular mobility by solid-state ^{13}C NMR spectroscopy

Hiroshi Miura^{a,*}, Makoto Kanebako^a, Hiroyuki Shirai^a, Hiroshi Nakao^a, Toshio Inagi^a, Katsuhide Terada^b

^a Fuji Research Laboratories, Pharmaceutical Division, Kowa Company Ltd., 332-1 Ohnoshinden, Fuji, Shizuoka 417-8650, Japan

^b Faculty of Pharmaceutical Sciences, Toho University, 2-2-1 Miyama, Funabashi, Chiba 274-8510, Japan

ARTICLE INFO

Article history:

Received 1 December 2010

Received in revised form 19 February 2011

Accepted 12 March 2011

Available online 21 March 2011

Keywords:

Porous silica

Amorphous

Relaxation time

Solid-state NMR

Raman spectroscopy

ABSTRACT

This study evaluated the physical stability and molecular mobility of a poorly water-soluble amorphous drug, 2-benzyl-5-(4-chlorophenyl)-6-[4-(methylthio)phenyl]-2H-pyridazin-3-one (K-832), adsorbed onto silica mesopores. K-832–Sylsilia 740 and K-832–Sylsilia 350 formulations, prepared by adsorbing K-832 onto porous silica Sylsilia 740 (2.5-nm-diameter pores) and Sylsilia 350 (21-nm-diameter pores) and stored at 60 °C/80%RH (open and closed conditions), were investigated. Differential scanning calorimetry revealed that crystallization of K-832 in the K-832–Sylsilia 350 formulation stored at 60 °C/80%RH (open and closed conditions) was faster than that of the other formulation stored under identical conditions. Raman spectroscopy revealed shifts to higher wavenumbers in the K-832–Sylsilia 350 and K-832–Sylsilia 740 formulations (1497 and 1493 cm^{-1} , respectively) in comparison to amorphous K-832 (1481 cm^{-1}); however, no distinct differences were observed in the spectra of the two formulations. Solid-state ^{13}C NMR spectroscopy revealed a difference in spin–lattice relaxation time in the rotating frame ($T_{1\rho}$) between the two formulations, suggesting the lower molecular mobility of K-832 in the 2.5-nm-diameter pores than in the 21-nm-diameter pores. Thus, the crystallization rate of amorphous K-832 in the K-832–Sylsilia 740 formulation was much slower. These results will be useful in estimating the physical stability of amorphous drugs in mesopores.

© 2011 Elsevier B.V. All rights reserved.

1. Introduction

For many years, the use of an amorphous form of a poorly water-soluble drug has been attracting considerable interest as a potential approach for improving the solubility and oral bioavailability of the drug. However, because an amorphous form is a physically unstable form, a drug in this form may undergo recrystallization during storage. Moreover, the dissolution rate of the drug changes with recrystallization. Therefore, the stabilization of drugs in amorphous forms is an active research area in the pharmaceutical field (Serajuddin, 1999).

It is important to evaluate the amorphous state of a drug precisely in order to ensure the quality and effectiveness of a pharmaceutical preparation. To this end, numerous analyses have been carried out by techniques such as powder X-ray diffractometry (PXRD), differential scanning calorimetry (DSC), isothermal

microcalorimetry, solution calorimetry, infrared spectroscopy, near-infrared spectroscopy, Raman spectroscopy, solid-state NMR spectroscopy, and thermally stimulated depolarization current analysis (Hirakura et al., 2007). However, in most of these techniques, assays performed for determining the amorphous content of a sample yield content values that are inferred from the degree of crystallinity of the sample. This is because these techniques detect the specific properties of crystalline samples, except a few techniques wherein the amorphous phase is predominantly detected (Shah et al., 2006). Accordingly, there is a requirement for the development of a new method for directly observing and evaluating an amorphous form.

In our previous studies, we investigated a new solid dispersion system for a poorly water-soluble drug, 2-benzyl-5-(4-chlorophenyl)-6-[4-(methylthio)phenyl]-2H-pyridazin-3-one (K-832 (Ohkuchi et al., 2002; Tabunoki et al., 2003)), in which a high-surface-area silica was used as a carrier and supercritical CO_2 was used as a solvent, and we demonstrated its applicability in the pharmaceutical field (Miura et al., 2010). In these studies, K-832 existed in the amorphous state because it was adsorbed onto

* Corresponding author. Tel.: +81 545 33 1716; fax: +81 545 33 1805.

E-mail address: h-miura@kowa.co.jp (H. Miura).

the high-surface-area silica; therefore, the dissolution and *in vivo* absorption of K-832 were enhanced. We also demonstrated that a drug–porous silica (Sylysia 350) formulation showed better drug absorption than a drug–nonporous silica (Aerosil 200) formulation (Miura et al., 2011). Porous silica, which was employed in our previous study, is commonly used as a pharmaceutical inactive ingredient and has numerous mesopores in its structure, i.e. pores with diameters between 2 and 50 nm. The molecular mobility of a drug in mesopores is expected to be different in mesopores of different sizes and is also expected to depend on the interaction between the drug and the mesopore wall. Decreased molecular mobility is expected to lead to the stabilization of drugs in amorphous forms. However, the physical stability and molecular mobility of an amorphous drug in mesopores have not yet been investigated in detail.

Therefore, the objective of this study was to evaluate the correlation between the physical stability and molecular mobility of amorphous K-832 in silica pores of different diameters by PXRD, DSC, Raman spectroscopy, and solid-state ^{13}C NMR spectroscopy.

2. Materials and methods

2.1. Materials

K-832 used in this study was manufactured by Kowa Company Ltd. Sylysia 740 and Sylysia 350 (Table 1) were supplied by Fuji Silysia Chemical Ltd. Dichloromethane (DCM, special grade reagent) was purchased from Wako Pure Chemical Industries Ltd.

2.2. Preparation of K-832–silica formulation by solvent method

First, 1.20 g K-832 was dissolved in 160 mL DCM; then, 6.80 g Sylysia 740 was dispersed in this solution (K-832:Sylysia 740 = 15:85 (w/w)), and the suspension was sonicated for 5 min. Subsequently, DCM was removed from the suspension. Thereafter, the residue was dried for 4 h at 30–35 °C under vacuum, thus yielding a K-832–Sylysia 740 formulation. In the case of Sylysia 350, the ratio of K-832 to Sylysia 350 was kept at 12:88 (w/w), thereby yielding a K-832–Sylysia 350 formulation. For comparison, physical mixtures (K-832–Sylysia 740 physical mixture and K-832–Sylysia 350 physical mixture) were also prepared (Table 2).

2.3. Stability test of amorphous state

A test for evaluating the stability of the amorphous state of the drug was conducted at 60 °C/80% relative humidity (RH). In this test, the K-832–Sylysia 740 and K-832–Sylysia 350 formulations were placed in both open and closed glass vials which were stored in a controlled-temperature environment (60 °C) inside a desiccator

containing saturated KCl solutions in order to generate appropriate RH. These formulations stored at 60 °C/80% RH were removed after two different periods of time—after 2 weeks and after 1 month—and tested for crystallinity by PXRD and DSC. In the PXRD measurement (Rigaku RINT2000, Japan), Cu K α radiation was used as the X-ray source. A sample was scanned from 5° to 35° (2 θ) at a scanning speed of 5°/min. The diffraction pattern was measured at a voltage of 40 kV and current of 20 mA. The DSC measurement (Shimadzu DSC-60, Japan) was performed at a heating rate of 10 °C/min. The sample chamber was purged with nitrogen (20 mL/min).

2.4. Measurement of Raman spectra

The Raman spectra of crystalline and amorphous K-832 and the K-832–Sylysia 740 and K-832–Sylysia 350 formulations were measured using an STR laser Raman system (Seki Technotron Corp., Japan). Scanning was carried out in the range of 4000–370 cm $^{-1}$. Amorphous K-832 for Raman spectroscopy was prepared by heating crystalline K-832 at 180 °C to melt it and then cooling the melted sample by immersing it in liquid nitrogen.

2.5. Measurement of solid-state ^{13}C NMR spectra and relaxation time

The solid-state ^{13}C NMR spectra of crystalline K-832, K-832–Sylysia 740 formulation, and K-832–Sylysia 350 formulation were measured using an AVANCE 300 MHz digital NMR (Bruker BioSpin, Japan) at a proton resonance frequency of 300.13 MHz. The samples were spun by a jet of dry air at the magic angle (54.7°) with a spinning rate of 5 kHz in the probe head (7 mm i.d.). The chemical shifts were externally referenced to the carbonyl signal of glycine at 176.03 ppm. The NMR data were analyzed using TopSpin ver1.3 (Bruker BioSpin, Japan).

In spectra obtained by cross polarization/magic angle spinning (CP/MAS) measurements, the signal ranges in which relaxation time was calculated (ranges 1–5) were decided (1, 160–168 ppm, C=O; 2, 145–154 ppm, C of aromatic ring; 3, 118–145 ppm, C of aromatic ring; 4, 53–63 ppm, CH $_2$; 5, 12–20 ppm, CH $_3$). The spin–lattice relaxation time in the rotating frame ($T_{1\rho}$) was determined at 27 °C. The maximum duration of the spin-locking field for the $T_{1\rho}$ measurement was 15 ms.

3. Results

3.1. Preparation of K-832–silica formulation by solvent method

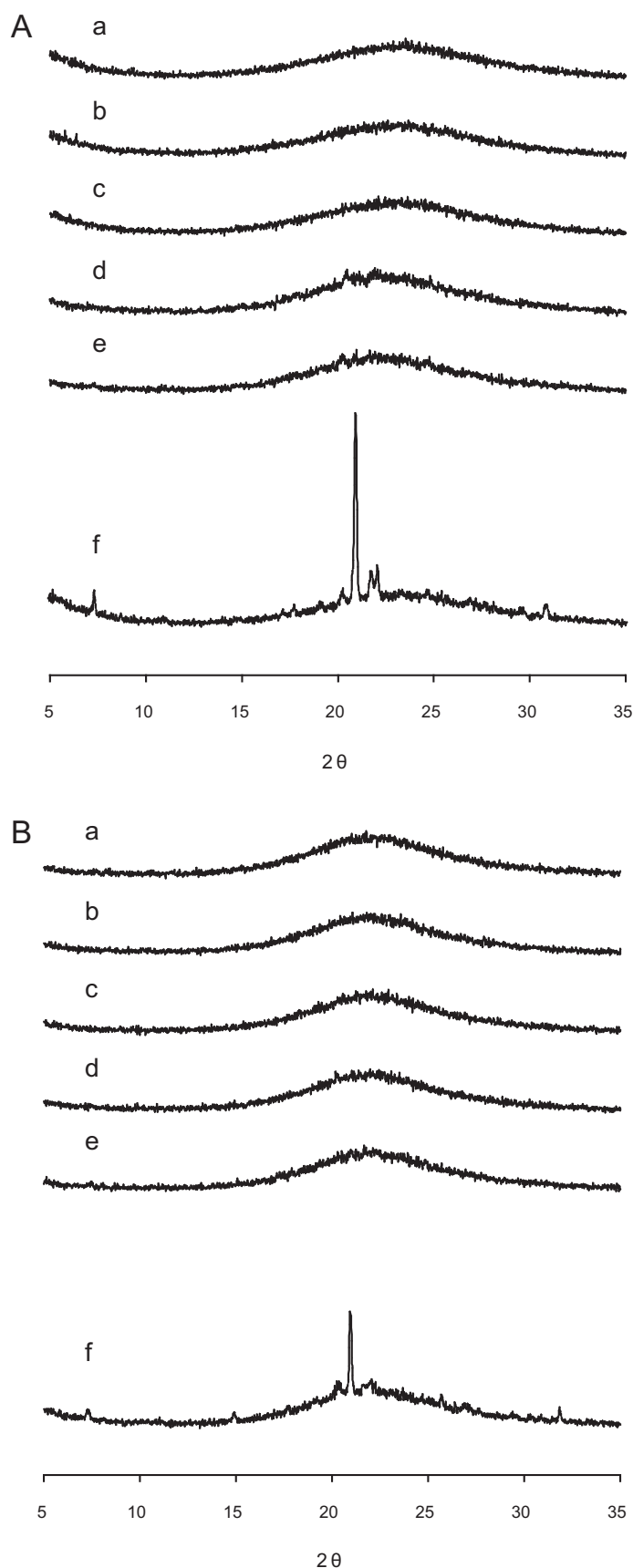
The ratio of K-832 to Sylysia 740 was 15:85 (w/w) and that to Sylysia 350 was 12:88 (w/w). When the ratio of K-832 to the silicas was increased beyond the abovementioned ratios, the crys-

Table 1
Physical properties of porous silica particles.

Sample	Structure type	Pore size (nm)	Pore volume (mL/g)	Specific surface area (m 2 /g)	Particle size (μm)
Sylysia 740	Porous structure	2.5	0.44	700	5.0
Sylysia 350	Porous structure	21.0	1.60	300	3.9

Table 2
Composition and formulation procedure for K-832–silica formulations and corresponding physical mixtures.

Formulation	Composition and ratio (w/w)			Formulation procedure
	K-832	Sylysia 740	Sylysia 350	
K-832–Sylysia 740 formulation	15.0	85.0	–	Adsorbing K-832 onto Sylysia 740 from dichloromethane solution
K-832–Sylysia 740 physical mixture	15.0	85.0	–	Physical mixture of K-832 with Sylysia 740
K-832–Sylysia 350 formulation	12.0	–	88.0	Adsorbing K-832 onto Sylysia 350 from dichloromethane solution
K-832–Sylysia 350 physical mixture	12.0	–	88.0	Physical mixture of K-832 with Sylysia 350



talline state of K-832 was retained in the obtained formulations, i.e. the formulations consisted of the amorphous and crystalline states of K-832. DSC measurements showed that the obtained K-832-Sylsya 740 and K-832-Sylsya 350 formulations did not have an endothermic peak at the K-832 melting point (155–159 °C); thus, K-832 ceased to exist in the crystalline state and was instead in the amorphous state. These formulations were used in the stability test of the amorphous state.

3.2. Stability test of amorphous state

Fig. 1 shows PXRD patterns of the physical mixtures and of the K-832-Sylsya 740 and K-832-Sylsya 350 formulations before and after storage. The physical mixtures (Fig. 1f) containing K-832 crystals showed distinctive diffraction peaks, which indicates the high crystallinity of K-832. The K-832-Sylsya 740 and K-832-Sylsya 350 formulations before storage did not have diffraction peaks and showed a halo pattern (Fig. 1a). The K-832-Sylsya 740 and K-832-Sylsya 350 formulations stored for 2 weeks and for 1 month in closed glass vials (i.e. under a closed condition) did not show the diffraction peaks, which indicates the existence of the crystalline state (Fig. 1b and c). In contrast, the K-832-Sylsya 740 and K-832-Sylsya 350 formulations stored for 2 weeks and for 1 month in open glass vials (i.e. under an open condition) showed diffraction peaks with low intensities (Fig. 1d and e).

The DSC curves of the K-832-Sylsya 740 and K-832-Sylsya 350 formulations before and after storage are shown in Fig. 2. The heat of fusion of these formulations is summarized in Table 3. The endothermic peak, which originated from the melting point of K-832 crystal, was not observed for the two formulations before storage (Fig. 2a). For the K-832-Sylsya 740 formulation, the peak was also not observed after storage at 60 °C/80% RH in closed glass vials for both 2 weeks and 1 month (Fig. 2(A), b and c). In contrast, for the K-832-Sylsya 350 formulation, two small peaks were observed after storage at 60 °C/80% RH in closed glass vials for 1 month (Fig. 2(B), c, -0.09 J/g). Furthermore, when these formulations were stored at 60 °C/80% RH under the open condition to ensure that they were affected by humidity, the endothermic peaks were observed for both formulations (Fig. 2d and e), and the peak intensities (i.e. the heat of fusion of the formulations) increased with the storage period (see Table 3). Broad peaks for the K-832-Sylsya 350 formulation (Fig. 2(B), d and e) were observed at a temperature lower than that for the K-832-Sylsya 740 formulation (Fig. 2(A), e). Further, for both durations (2 weeks and 1 month), the heat of fusion of the K-832-Sylsya 350 formulation was greater than that of the K-832-Sylsya 740 formulation.

3.3. Raman spectra

Fig. 3 shows the Raman spectra of crystalline and amorphous K-832, K-832-Sylsya 740 formulation, and K-832-Sylsya 350 formulation (1800 – 1300 cm^{-1}). It was observed that amorphous K-832 showed a shift to a higher wavenumber (1481 cm^{-1}) in comparison to crystalline K-832 (1474 cm^{-1}); a reduction in intensity (1408 cm^{-1}) was also observed with a change from the crystalline form to the amorphous form. The spectra of the K-

Fig. 1. Powder X-ray diffraction patterns of physical mixtures and of K-832-Sylsya 740 formulation and K-832-Sylsya 350 formulation before and after storage at 60 °C/80% RH. (A) K-832-Sylsya 740 (2.5 nm); (B) K-832-Sylsya 350 (21 nm); a, before storage; b, after storage under closed condition for 2 weeks; c, after storage under closed condition for 1 month; d, after storage under open condition for 2 weeks; e, after storage under open condition for 1 month; f, physical mixture.

Table 3
Heat of fusion of K-832–Sylysia 740 formulation and K-832–Sylysia 350 formulation.

Sample	Heat of fusion (J/g)				
	Before storage	60 °C/80%RH, closed condition		60 °C/80%RH, open condition	
		2 weeks	1 month	2 weeks	1 month
K-832–Sylysia 740 formulation	0	0	0	−0.09(127.5, 151.3 °C)	−0.24 (153.8 °C)
K-832–Sylysia 350 formulation	0	0	−0.09(139.0, 151.7 °C)	−1.04 (147.8 °C)	−1.89(147.0, 154.5 °C)

832–Sylysia 350 and K-832–Sylysia 740 formulations were similar to that of amorphous K-832 in the range of 1420–1370 cm^{−1}; the K-832–Sylysia 350 and K-832–Sylysia 740 formulations showed further shifts to higher wavenumbers (1497 cm^{−1} and 1493 cm^{−1}, respectively) in comparison to amorphous K-832 (1481 cm^{−1}). However, no obvious difference was observed between the spectra of the K-832–Sylysia 350 formulation and the K-832–Sylysia 740 formulation.

3.4. Solid-state ¹³C NMR spectra

The chemical structure of K-832 and solid-state ¹³C NMR spectra of crystalline K-832, the K-832–Sylysia 740 formulation, and K-832–Sylysia 350 formulation are shown in Fig. 4(A) and (B), respectively. The signals in the spectra of the K-832–Sylysia 740 and K-832–Sylysia 350 formulations were found to be broader than those in the spectrum of crystalline K-832. In the spectrum of crystalline K-832, chemical shifts of carbon C_a, C_b, and C_c (see Fig. 4(A)) were observed at 161.4, 59.6, and 14.0 ppm, respectively. In contrast, in the spectrum of the K-832–Sylysia 740 formulation, the chemical shifts of carbon C_a and C_c were observed at 163.5 and 15.6 ppm, respectively. In the spectrum of the K-832–Sylysia 350 formulation, these chemical shifts were observed at 163.0 and 15.1 ppm, respectively. Consequently, the lower-field shifts of these carbons were observed in the spectra of the two formulations. The shifts of carbon C_b in both the formulations were not determined, because the spectral patterns for this carbon in both formulations showed broad signals.

3.5. Relaxation time

Fig. 5 shows the *T*_{1ρ} values of the respective signal ranges (1–5) for K-832 in the K-832–Sylysia 740 and K-832–Sylysia 350 formulations. The *T*_{1ρ} values of signal ranges 1 (C=O), 2 (Ar), 3 (Ar), and 5 (CH₃), i.e. with the exception of signal range 4 (CH₂), for K-832 in the former formulation were larger than those in the latter formulation. These results indicated that K-832 in the former formulation, whose carrier had a pore diameter of 2.5 nm, showed slower relaxation than K-832 in the latter formulation, whose carrier had a pore diameter of 21 nm.

4. Discussion

Porous silica is generally prepared by acid deposition from Na₂SiO₃ solution or by a sol–gel method from silicic acid esters. Porous silica with different pore diameters, pore volumes, and specific surface areas can be obtained by changing the preparation conditions (Takeuchi, 1999). In this study, we focused only on the pore diameter of porous silica and used Sylysia 740 and Sylysia 350 with pore diameters of 2.5 and 21 nm, respectively, as drug carriers.

The PXRD results of the K-832–Sylysia 740 and K-832–Sylysia 350 formulations stored at 60 °C/80% RH for 2 weeks and for 1 month in closed glass vials did not show diffraction peaks; this observation suggests that it was difficult to crystallize amorphous K-832, which existed in the mesopores of silica, under high-temperature conditions. However, under high-humidity conditions (80% RH, open condition), even though the peak strengths of the formulations stored for 2 weeks and for 1 month were smaller than

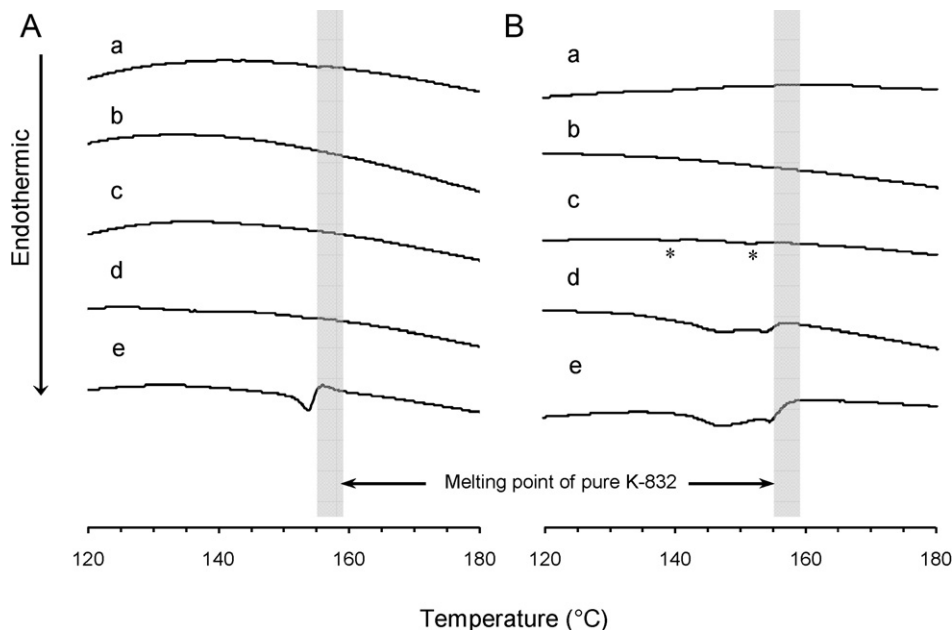


Fig. 2. DSC curves of K-832–Sylysia 740 formulation and K-832–Sylysia 350 formulation before and after storage at 60 °C/80% RH. (A) K-832–Sylysia 740 (2.5 nm); (B) K-832–Sylysia 350 (21 nm); a, before storage; b, after storage under closed condition for 2 weeks; c, after storage under closed condition for 1 month; d, after storage under open condition for 2 weeks; e, after storage under open condition for 1 month. *A small peak is observed.

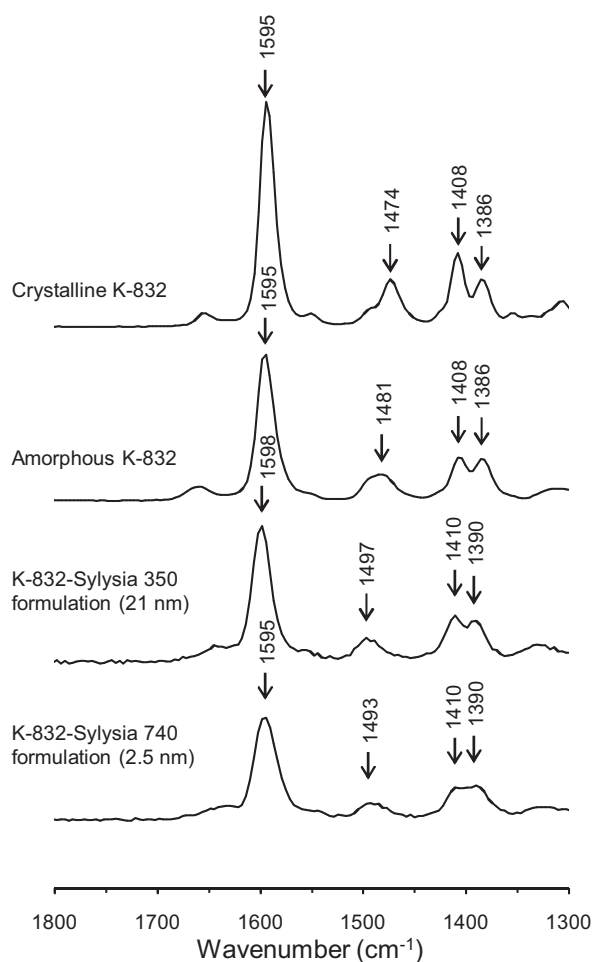


Fig. 3. Raman spectra of crystalline and amorphous K-832, K-832–Sylsilia 350 formulation, and K-832–Sylsilia 740 formulation.

that of the physical mixture, the formulations showed small peaks at around $20\text{--}25^\circ$. When the peak intensity measured by PXRD is very small, only a limited amount of information can be obtained from the PXRD pattern. Therefore, it was seemingly difficult to precisely compare the physical stabilities of the two formulations by PXRD measurements, because of the small peak intensities.

Many researchers have evaluated high-surface-area material–drug systems by PXRD and DSC measurements to elucidate crystallinity, crystalline polymorph, and physical stability of drugs. In our study, because it was difficult to perform a detailed comparison of the physical stabilities by PXRD measurement (for the reason mentioned above), we attempted to carry out a comparison of physical stabilities by DSC. DSC measurements showed that the peak intensity (the heat of fusion of the formulations), which increased with the storage period, of the K-832–Sylsilia 740 formulation was smaller than that of the K-832–Sylsilia 350 formulation (Table 3); this result suggested that the adsorption of K-832 onto Sylsilia 740, which has much smaller mesopores (2.5 nm), resulted in higher physical stability of amorphous K-832 than its adsorption onto Sylsilia 350, with a pore diameter of 21 nm. Further, the DSC curve of the K-832–Sylsilia 740 formulation stored at $60^\circ\text{C}/80\%$ RH under the open condition for 1 month was the same as the curve for crystalline K-832, albeit with much lower intensity. This fact implies that amorphous K-832 undergoes crystallization during storage under the high-humidity condition. A K-832 molecule has a diameter of approximately

1.3 nm. The pore diameter of Sylsilia 740 (2.5 nm) is insufficient for the proper growth of crystals of K-832; therefore, it seems that in the presence of water around the formulation, some of the K-832 molecules moved from the pores to the silica particle surface and subsequently crystallized on the surface. In contrast, in the case of the K-832–Sylsilia 350 formulation stored at $60^\circ\text{C}/80\%$ RH under the open condition for both 2 weeks and 1 month, a broad endothermic peak was observed at a temperature lower than the melting point of crystalline K-832 ($155\text{--}159^\circ\text{C}$). This result can possibly be attributed to the fact that several molecules form a cluster of K-832 in Sylsilia 350, with a pore diameter of 21 nm. Therefore, the cluster of K-832 was observed to melt at a temperature lower than the fusion temperature of crystalline K-832. From this behaviour, it can be said that not only the physical stability of an amorphous drug but also the existence state of the drug formed from the amorphous state during storage of the formulation is different for different pore diameters of the silica.

It is well recognized that the crystallization of an amorphous drug is promoted by humidity (Andrews et al., 2010; Andronis et al., 1997; Hancock and Zografi, 1997). On the basis of our results listed in Table 3, we can say that the amorphous drug in the silica pores in our system was also affected by humidity. However, a comparison of the extent of crystallization of the amorphous drug in the K-832–silica system with that of a general solid dispersion system consisting of K-832 and a water-soluble polymer (hydroxypropylmethylcellulose) as a carrier, as evaluated by DSC, revealed that the extent of crystallization in the K-832–silica system was clearly much lower than that in the solid dispersion system (Miura, unpublished data). Therefore, we can conclude that our approach of stabilizing drugs in amorphous forms by using the mesopores of silica was effective.

In this study, we also carried out Raman spectroscopy of crystalline and amorphous K-832 and the two formulations in order to investigate the state of existence of the drug molecules; furthermore, we investigated the interaction of drugs with porous silica (Fig. 3). Amorphous K-832 showed a shift to a higher wavenumber (1481 cm^{-1}) in comparison to crystalline K-832 (1474 cm^{-1}); this shift was accompanied by a reduction in intensity (1408 cm^{-1}), and these observations suggested the disruption of the highly ordered crystal lattice of K-832. In addition, the K-832–Sylsilia 350 formulation (1497 cm^{-1}) and K-832–Sylsilia 740 formulation (1493 cm^{-1}), in which K-832 existed in the amorphous state (as observed by PXRD and DSC measurements), showed further shifts to a higher wavenumber in comparison to amorphous K-832 (1481 cm^{-1}); these shifts were assumed to be caused by the highly disordered state of drugs resulting from the presence of mesopores. Thus, Raman spectroscopy revealed that the molecular environment of amorphous K-832 in the formulations (i.e. amorphous K-832 in the mesopores of silica) was different from that of the amorphous K-832 alone. In general, the formation of hydrogen bonds within a given system may be identified through a red shift in the absorption band (shift to a lower wavenumber), band broadening, and/or peak intensification (Andrews et al., 2010). In this system, the red shift and peak intensification were not observed in the spectra shown in Fig. 3. Thus, we considered that the silanol groups on the silica surface did not form hydrogen bonds with the K-832 molecules. Raman spectroscopy showed that there was no clear difference between the spectra of the K-832–Sylsilia 350 and K-832–Sylsilia 740 formulations. Therefore, we could evaluate the difference between crystalline K-832, amorphous K-832, and K-832–silica formulations by Raman spectroscopy; however, we found it difficult to detect the difference between the states of existence of the drug in 2.5-nm pores and 21-nm pores by Raman spectroscopy.

Then, we carried out solid-state ^{13}C NMR spectroscopy of crystalline K-832 and the two formulations in order to investigate the difference between the states of existence of the drug molecules

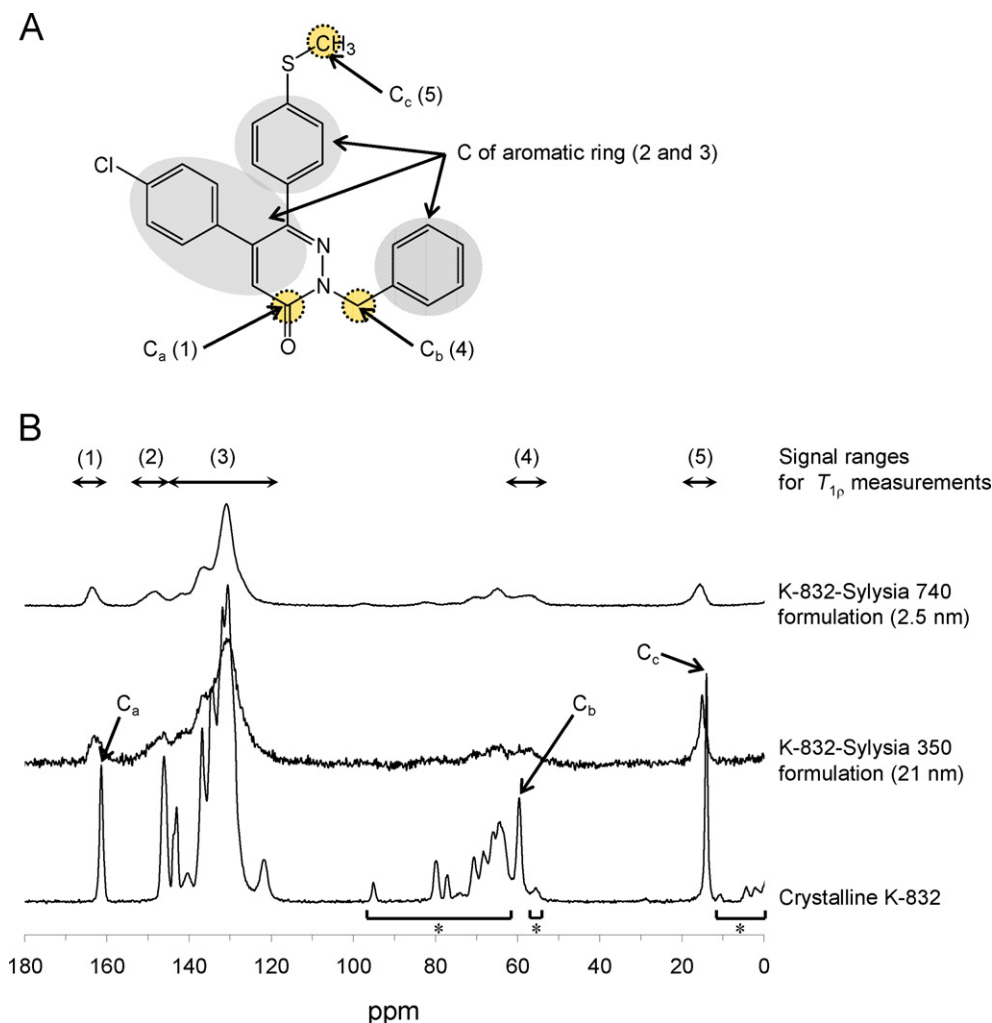


Fig. 4. Chemical structure of K-832 (A), solid-state ¹³C NMR spectra of K-832–Sylsilia 740 formulation, K-832–Sylsilia 350 formulation, crystalline K-832 (B), and signal ranges for $T_{1\rho}$ measurement (B). Spinning sidebands are marked with asterisks. Signal range no. 1, 160–168 ppm, C=O; 2, 145–154 ppm, C of aromatic ring; 3, 118–145 ppm, C of aromatic ring; 4, 53–63 ppm, CH₂; 5, 12–20 ppm, CH₃.

in mesopores with different pore diameters (Fig. 4). The solid-state ¹³C NMR spectra showed lower-field shifts for carbon C_a and C_c in the spectra of the K-832–Sylsilia 740 and K-832–Sylsilia 350 formulations. These results imply that the molecular state of K-832 in the formulations was different from that of crystalline K-832. As a result, it can be said that the molecular mobility of the drug changed with its adsorption onto silica. Aso et al. (2001) revealed that the crystallization of amorphous nifedipine and phenobarbital was largely correlated with their molecular mobilities by the mean relaxation time study of amorphous compounds, which was based on the Adam–Gibbs–Vogel equation. Moreover, in the past several years, solid-state ¹³C NMR spectroscopy has been used to evaluate the molecular mobility of drugs (Aso et al., 2001; Gonnella et al., 2010; Koga et al., 2004; Lubach et al., 2007; Masuda et al., 2005). Masuda et al. (2005) also concluded that the difference in the molecular mobilities of two amorphous compounds (indomethacin and salicin), which were based on the spin–lattice relaxation time measured by solid-state ¹³C NMR spectroscopy, was correlated with the crystallization behaviour of the two compounds. However, the past reports related to the measurement of a single component. It would be interesting to extend these measurements to multicomponent systems and to ascertain whether the molecular mobility of amorphous drugs in mesopores would be different for different pore diameters. Therefore, in this study, to gain initial insight into

the difference in physical stabilities of amorphous drugs in mesopores of different diameters, the $T_{1\rho}$, which was considered as a measure of molecular mobility (Aso et al., 2001), was determined for the K-832–Sylsilia 740 and K-832–Sylsilia 350 formulations. It should be emphasized that the $T_{1\rho}$ values of these two formulations were found to be different (Fig. 5). These results suggested that the molecular mobility of K-832 in the 2.5-nm-diameter pores was lower than that in the 21-nm-diameter pores. Therefore, we considered that the crystallization rate of amorphous K-832 in the 2.5-nm-diameter pores (i.e. K-832–Sylsilia 740 formulation) was much slower. This prediction is in agreement with the results of the stability test, in which it was found that the heat of fusion (which increased during storage) of the K-832–Sylsilia 740 formulation was smaller than that of the K-832–Sylsilia 350 formulation for each storage period. Therefore, we think that these results provided by solid-state ¹³C NMR measurements could serve as useful information for estimating the physical stability of an amorphous drug in mesopores in the case of a multicomponent drug–silica system. Using solid-state ¹³C NMR spectroscopy as an evaluation technique for the drug–silica system in this study is advantageous in that no interference peak originated from the silica (SiO₂) used as the drug carrier, because of which the analysis is simplified. We can also conclude that the 2.5-nm-diameter mesopores are better suited for ensuring the stability of amorphous K-832.

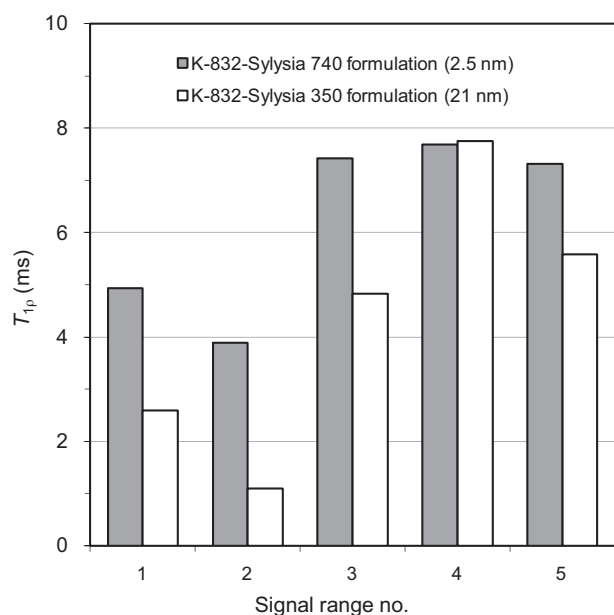


Fig. 5. Comparison of $T_{1\rho}$ of K-832-Sylsia 740 formulation and K-832-Sylsia 350 formulation.

5. Conclusions

The physical stability and molecular mobility of a poorly water-soluble amorphous drug, 2-benzyl-5-(4-chlorophenyl)-6-[4-(methylthio)phenyl]-2H-pyridazin-3-one (K-832), adsorbed onto silica mesopores, were evaluated. In the stability test, it was difficult to accurately compare the physical stabilities of the two solid dispersion systems containing porous silica with mesopores of different diameters (2.5 nm and 21 nm) by PXRD measurements, because of the small peak intensities. DSC measurements showed that the peak intensity (i.e. the heat of fusion), of the K-832-Sylsia 740 formulation, which increased with the storage period, was smaller than that of the K-832-Sylsia 350 formulation. This result suggests that the adsorption of K-832 onto Sylsia 740, which has much smaller mesopores (2.5 nm), was responsible for the higher physical stability of amorphous K-832. On the basis of the DSC results, we believed that not only the physical stability of an amorphous drug but also the existence state of the drug formed from the amorphous state during storage of the formulation was different for different pore diameters of silica. Raman spectroscopy revealed that the molecular environment of amorphous K-832 in the mesopores of silica was different from that of amorphous K-832 alone. However, it was difficult to detect the difference between the states of existence of the drug in 2.5-nm pores and 21-nm pores by Raman spectroscopy. In the relaxation time study using solid-state ^{13}C NMR, the investigation of $T_{1\rho}$ —used as a measure of molecular mobility—of amorphous K-832 in the two formulations revealed that the molecular mobilities of K-832 in mesopores of these two diameters were different. The larger $T_{1\rho}$ values in the case of carbon environments in the 2.5-nm pores suggested that the molecular mobility of K-832 in these pores was lower than that in the 21-nm pores. Therefore, we thought that the crystallization rate of amorphous K-832 in the 2.5-nm pores might be much slower. This

prediction was in agreement with the results of the stability test, where we found that the heat of fusion (which increased during storage owing to the recrystallization) of the K-832-Sylsia 740 formulation (2.5 nm) was smaller than that of the K-832-Sylsia 350 formulation (21 nm) for each storage period. On the basis of all these results, we conclude that the 2.5-nm mesopores are better suited for ensuring the stability of amorphous K-832. We believe that solid-state ^{13}C NMR measurements in multicomponent drug-silica systems can provide information that would be useful for pharmaceutical research and development.

Acknowledgements

The authors thank Miss. Minako Takagi (Faculty of Pharmaceutical Sciences, Toho University) for her assistance in the solid-state NMR spectroscopy. The authors also acknowledge Fuji Silysia Chemical Ltd. (Aichi, Japan) for providing the porous silica used in the study.

References

- Andrews, G.P., AbuDiak, O.A., Jones, D.S., 2010. Physicochemical characterization of hot melt extruded bicalutamide-polyvinylpyrrolidone solid dispersions. *J. Pharm. Sci.* 99, 1322–1335.
- Andronis, V., Yoshioka, M., Zografi, G., 1997. Effects of sorbed water on the crystallization of indomethacin from the amorphous state. *J. Pharm. Sci.* 86, 346–351.
- Aso, Y., Yoshioka, S., Kojima, S., 2001. Explanation of the crystallization rate of amorphous nifedipine and phenobarbital from their molecular mobility as measured by ^{13}C nuclear magnetic resonance relaxation time and the relaxation time obtained from the heating rate dependence of the glass transition temperature. *J. Pharm. Sci.* 90, 798–806.
- Gonnella, N.C., Smoliga, J.A., Campbell, S., Busacca, C.A., Cerreta, M., Var-solona, R., Norwood, D.L., 2010. Study and characterization of crystalline hydrate/polymorph forms of 5,11-dihydro-11-ethyl-5-methyl-8-(2-(1-oxido-4-quinolinyl)ethyl-6H-dipyrro(3,2-B:2',3'-E)(1,4)diazepin-6-one by solid-state NMR and solution NMR. *J. Pharm. Biomed. Anal.* 51, 1047–1053.
- Hancock, B.C., Zografi, G., 1997. Characteristics and significance of the amorphous state in pharmaceutical systems. *J. Pharm. Sci.* 86, 1–12.
- Hirakura, Y., Yamaguchi, H., Mizuno, M., Miyaniishi, H., Ueda, S., Kitamura, S., 2007. Detection of lot-to-lot variations in the amorphous microstructure of lyophilized protein formulations. *Int. J. Pharm.* 340, 34–41.
- Koga, A., Yonemochi, E., Machida, M., Aso, Y., Ushio, H., Terada, K., 2004. Microscopic molecular mobility of amorphous AG-041R measured by solid-state ^{13}C NMR. *Int. J. Pharm.* 275, 73–83.
- Lubach, J.W., Xu, D., Segmuller, B.E., Munson, E.J., 2007. Investigation of the effects of pharmaceutical processing upon solid-state NMR relaxation times and implications to solid-state formulation stability. *J. Pharm. Sci.* 96, 777–787.
- Masuda, K., Tabata, S., Sakata, Y., Hayase, T., Yonemochi, E., Terada, K., 2005. Comparison of molecular mobility in the glassy state between amorphous indomethacin and salicin based on spin-lattice relaxation times. *Pharm. Res.* 22, 797–805.
- Miura, H., Kanabako, M., Shirai, H., Nakao, H., Inagi, T., Terada, K., 2010. Enhancement of dissolution rate and oral absorption of a poorly water-soluble drug, K-832, by adsorption onto porous silica using supercritical carbon dioxide. *Eur. J. Pharm. Biopharm.* 76, 215–221.
- Miura, H., Kanabako, M., Shirai, H., Nakao, H., Inagi, T., Terada, K., 2011. Influence of particle design on oral absorption of poorly water-soluble drug in a silica particle-supercritical fluid system. *Chem. Pharm. Bull.* in press.
- Ohkuchi, M., Kyotani, Y., Shigyo, H., Koshi, T., Kitamura, T., Ohgiya, T., Matsuda, T., Yamazaki, Y., Kumai, N., Kotaki, K., Yoshizaki, H., Habata, Y., 2002. Pyridazine compounds and compositions containing the same. US patent 6,348,468.
- Serajuddin, A.T.M., 1999. Solid dispersion of poorly water-soluble drugs: early promises, subsequent problems, and recent breakthroughs. *J. Pharm. Sci.* 88, 1058–1066.
- Shah, B., Kakumanu, V.K., Bansal, A.K., 2006. Analytical techniques for quantification of amorphous/crystalline phases in pharmaceutical solids. *J. Pharm. Sci.* 95, 1641–1665.
- Tabunoki, Y., Edano, T., Murakami, K., Kobayashi, H., Koshi, T., Ohkuchi, M., Ohshima, S., Mima, T., Ishii, T., Hattori, Y., Saeki, Y., 2003. Anti-arthritis effects of a novel anti-cytokine low molecular weight compound, K-832. *Arthritis Rheum.* 48.
- Takeuchi, Y., 1999. Porous materials – characterization, production and application. Fuji Technosystem Co., Ltd., Japan.